ISSN 0023-1584, Kinetics and Catalysis, 2008, Vol. 49, No. 3, pp. 446–450. © MAIK "Nauka/Interperiodica" (Russia), 2008.
Original Russian Text © V.L. Volkov, E.I. Andreikov, G.S. Zakharova, V.Yu. Gavrilov, V.V. Kaichev, V.I. Bukhtiyarov, 2008, published in Kinetika i Kataliz, 2008, Vol. 49, No. 3, pp. 468–472.

Vanadium–Titanium Oxides: Sol–Gel Synthesis and Catalytic Properties in Chlorobenzene Oxidation

V. L. Volkov[a], E. I. Andreikov[b], G. S. Zakharova[a], V. Yu. Gavrilov[c], V. V. Kaichev[c], and V. I. Bukhtiyarov[c]

[a] *Institute of Solid-State Chemistry, Ural Branch, Russian Academy of Sciences, Yekaterinburg, 620219 Russia*
[b] *Postovskii Institute of Organic Synthesis, Ural Branch, Russian Academy of Sciences, Yekaterinburg, 620219 Russia*
[c] *Boreskov Institute of Catalysis, Siberian Branch, Russian Academy of Sciences, Novosibirsk, 630090 Russia*
e-mail: volkov@ihim.uran.ru

Received June 8, 2007

Abstract—Vanadium–titanium mixed oxides with V/Ti = 0.025, 0.050, and 0.100 have been synthesized by sol–gel processing. The anatase–rutile transition temperature decreases from 750 to 600°C as the vanadium content of the TiO_2 phase is increased. The most important texture parameters and the photoelectron and IR spectra of the oxides are reported. The oxides exhibit high catalytic activity in chlorobenzene oxidation, which is due to their specific electronic and crystal structures.

DOI: 10.1134/S0023158408030208

Vanadium–titanium mixed oxides are efficient commercial catalysts for the selective oxidation of *o*-xylene into phthalic anhydride [1, 2]. In recent decades, they have found use in solving the challenging environmental problem of removing organochlorine compounds from waste gases [3–5]. The properties of these oxides depend on the synthesis method because of structure effects. In the interaction between titanium dioxide powder and a vanadium salt solution, vanadium stays on the titanium dioxide surface and its incorporation into the TiO_2 lattice is hampered. This drawback can be eliminated by the sol–gel synthesis of the vanadium–titanium oxides [6–8]. In this case, vanadium ions can occur both on the surface and in the bulk of TiO_2. Therefore, the distribution of vanadium–oxygen active groups in the titanium dioxide matrix and, accordingly, the properties of the resulting catalyst depend strongly on the synthesis conditions. Chlorobenzene oxidation can yield volatile vanadium chlorides on the TiO_2 surface, and this can deactivate the catalyst. In order to rule out this process, it is necessary to employ solid solutions in which vanadium is in the titanium dioxide bulk.

Here, we report the synthesis, structure, texture parameters, and catalytic properties of vanadium–titanium mixed oxides.

EXPERIMENTAL

The starting chemicals were titanyl sulfate ($TiOSO_4 \cdot 2H_2O$), vanadium(V) oxide (V_2O_5), 30% hydrogen peroxide, and aqueous ammonia. All the chemicals were analytical grade. Stoichiometric amounts of $TiOSO_4 \cdot 2H_2O$ and V_2O_5 were dissolved in water and hydrogen peroxide, respectively. A stoichiometric amount of NH_4OH was added to the titanyl sulfate solution to obtain titanium hydroxide. The peroxide solution of vanadium was added to the resulting suspension, and the mixture was held at 60°C until the complete decomposition of the peroxide compounds. The resulting precipitate was filtered, washed with water, air-dried, and calcined for 10 h at 450°C. It was established by chemical analysis that the actual V/Ti ratio in these samples is equal to the preset ratio within ±0.004. In catalyst preparation by impregnation, we used anatase with unit cell parameters of $a = 3.778 \pm 0.001$ Å and $c = 9.486 \pm 0.004$ Å and a specific surface area of 63 m^2/g. TiO_2 powder was placed into an NH_4VO_3 solution (powder/liquid = 1 : 5 vol/vol), and the mixture was stirred at 70°C until a paste was obtained. The paste was dried at 95–100°C and was calcined at 450°C for 10 h.

Phase analysis was carried out on a DRON-2 diffractometer (CuK_α radiation). Morphology was studied using an LEO-982 scanning electron microscope (Carl Zeiss). The porous structure of V–Ti–O samples was studied by low-temperature (77 K) nitrogen adsorption using a DigiSorb-2600 Micromeritics instrument. The mesopore volume distribution over pore size was derived from the desorption branch of the isotherm by the Barrett–Joyner–Halenda (BJH) method [9]. The chemical composition of catalyst surfaces was determined on a VG ESCALAB HP electron spectrometer using nonmonochromated AlK_α radiation ($h\nu$ = 1486.6 eV). The binding energy scale was calibrated against the Au4$f_{7/2}$ (84.00 eV) and Cu2$p_{3/2}$ (932.67 eV) lines in the spectra of gold and copper foils, respectively. The relative amounts of elements in the analysis zone (surface layer 2–3 nm in thickness) were derived from the integrated intensities of XPS lines taking into

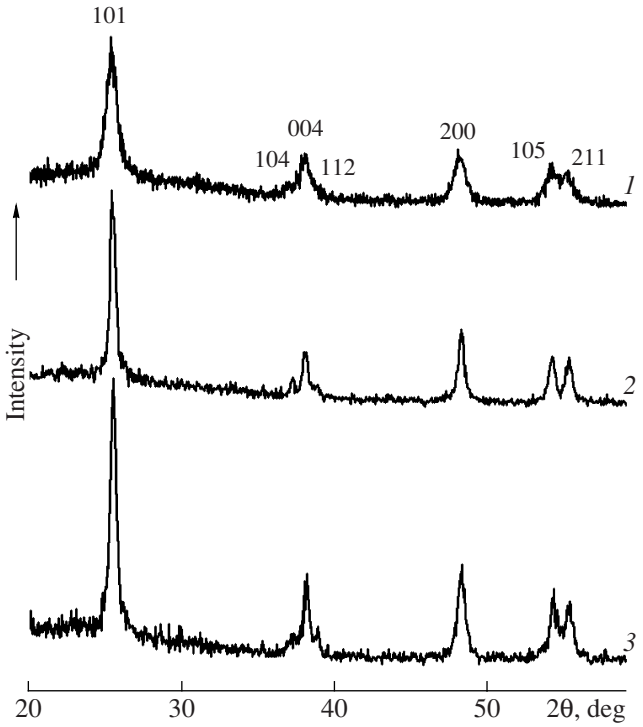

Fig. 1. Diffraction patterns from oxides with V/Ti = (*1*) 0.025, (*2*) 0.050, and (*3*) 0.100 calcined at T = (*1*) 700, (*2*) 600, and (*3*) 550°C.

account the corresponding atomic sensitivity factors [10]. For detailed chemical analysis, the spectra were deconvolved into its components. After background subtraction by the Shirley method [11], the experimental curve was separated into a number of lines corresponding to the photoemission of electrons from the inner levels of atoms in different chemical environments. The IR spectra of air-dry powders were recorded on a Spectrum spectrophotometer (Perkin-Elmer) with a resolution of ±2 cm^{-1}.

The catalytic properties of oxides in chlorobenzene oxidation were studied in a flow glass reactor in the temperature range of 290–460°C. An oxide powder (0.5 g) mixed with silicon carbide (1 : 2 vol/vol, particle size of ≥0.25 mm) was charged into the reactor, the reactor was brought to the preset temperature, and a vapor–air mixture with a chlorobenzene concentration of 40×10^{-5} mol/l was fed into the reactor. The GHSV of the mixture was 20000 h^{-1}. Partial chlorobenzene oxidation products were identified chromatographically. The total amount of CO and CO_2 was determined gravimetrically as CO_2 adsorbed on ascarite after the oxidation of CO into CO_2 on manganese dioxide at 300°C. Carbon oxides, HCl, and H_2O were detected as chlorobenzene oxidation products.

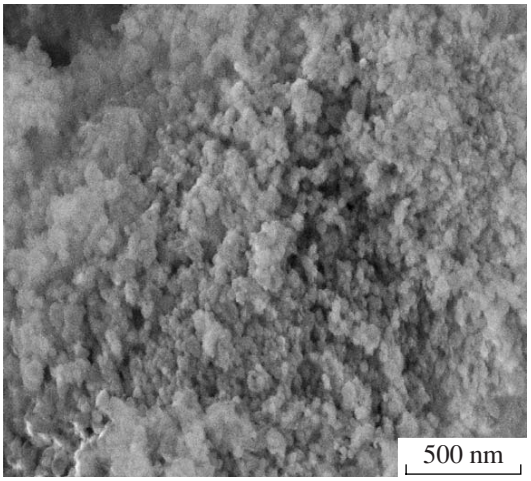

Fig. 2. Surface morphology of the V/Ti = 0.100 oxide.

RESULTS AND DISCUSSION

All vanadium–titanium oxide samples calcined at 400–450°C have the anatase structure. The thermal stability of this structure decreases as the vanadium content is increased. The anatase–rutile transition in the V/Ti = 0.025, 0.050, and 0.100 samples begins near 750, 650, and 600°C, respectively (Fig. 1). The unit cell parameters of the oxides calcined at 450°C are listed in Table 1.

The increase in the thermal stability of anatase at small extents of substitution of vanadium for titanium is due to the decrease in the unit cell parameters a and c. At V/Ti = 0.100, these parameters take substantially larger values, reducing the rutile structure formation temperature. According to scanning electron microscopy (SEM) data (Fig. 2), the mean particle size of the V/Ti = 0.100 powder is 20–30 nm.

Table 2 lists the texture parameters of the oxides, namely, the specific surface area (S_{BET}), the mesopore volume (V_s), and the dominant pore size (D). Figure 3 plots the mesopore volume distribution over pore size for different V/Ti ratios. It follows from these results that, as the vanadium content of the solid solution is raised, the specific surface area and the volume of the mesopores (~13 nm) decrease and the dominant pore size increases. Therefore, by varying the V/Ti ratio, it is possible to change the texture parameters of the oxides.

Table 1. Unit cell parameters of the titanium–vanadium mixed oxides calcined at 450°C

V/Ti	Unit cell parameter, Å	
	$a \pm 0.002$	$c \pm 0.005$
0.025	3.765	9.402
0.050	3.762	9.396
0.100	3.773	9.456

Table 2. Basic properties of the titanium–vanadium mixed oxides and element concentrations from XPS data

V/Ti	S_{BET}, m^2/g	V_s, cm^3/g	D, nm	V, wt %	[V]/[Ti]	[O]/[V + Ti]
0.025	159	0.447	7.4	2.59	0.10	2.56
0.050	152	0.449	9.2	5.05	0.16	2.49
0.100	131	0.417	11.8	9.60	0.30	2.50

This finding is of importance from the standpoint of catalytic activity.

The photoelectron spectra of the oxides show well-defined lines from the main constituent elements of the materials (Ti, V, and O) and indicate the presence of minor amounts of carbon (Fig. 4). The Ti2*p* spectrum consists of two peaks at 458.9 and 464.5 eV, which are due to the Ti2$p_{3/2}$–Ti2$p_{1/2}$ doublet. These data correlate well with data obtained for tetravalent titanium [12, 13]. The sharp O1*s* peak at 530.3–530.1 eV is due to main structural oxygen. Similar O1*s* binding energies for oxygen in TiO_2 were reported in an earlier publication [13].

It is difficult to analyze the V2*p* spectra because of the low vanadium concentration and the overlap of the V2$p_{3/2}$ and V2$p_{1/2}$ lines with the $K_{\alpha 3,4}$ O1*s* satellites. In order to obtain more reliable results, it is necessary to use monochromated radiation and a sample charge compensation system. The deconvolution of the V2*p* spectra into their components is presented in Fig. 5. Clearly, the V2$p_{3/2}$ line shifts slightly as the vanadium content is varied. For the V/Ti = 0.100 sample, which is the richest in vanadium, the V2$p_{3/2}$ line occurs at 516.9 eV, the binding energy characteristic of vanadium(V). According to the literature, the V2$p_{3/2}$ line for V_2O_4 and V_2O_5 occurs at 516.2–516.6 and 516.9–517.2 eV, respectively [14, 15]. For the V/Ti = 0.050 and 0.025 samples, the V2$p_{3/2}$ line is observed at 516.6 and 516.4 eV, the binding energies characteristic of V^{4+}. Therefore, when present at low concentrations, vanadium in the mixed oxides is mainly in the V^{4+} state. At higher vanadium contents, V^{5+} mainly forms during the synthesis.

The relative amounts of the elements in the surface layer (2–3 nm in thickness) of the solid solutions as derived from the integrated intensities of XPS lines are listed in Table 2. Clearly, the vanadium concentration in the surface layer and the bulk vanadium concentration are linearly correlated. However, the concentration of vanadium atoms in the surface layer is nearly three times higher than the bulk vanadium concentration. According to XPS data, the amount of oxygen on the surface exceeds the amount of oxygen necessary for the formation of a solid solution of V_2O_5 in TiO_2. This can be due to the high chemisorption capacity of the mixed oxides.

The structure of the mixed oxides was studied by IR spectroscopy using the vanadium-richest sample (V/Ti = 0.100) as an example. The asymmetric vibrations of the titanium–oxygen octahedra manifest themselves as a sharp absorption peak near 808 cm^{-1}. The stretching vibrations of the short terminal Ti–O bonds give rise to a broad band with a minimum at 731 cm^{-1}. The bending and asymmetric vibrations of the Ti–O–Ti bridges are observed at 659 and 536 cm^{-1}, respectively. The stretching vibrations of bonds with different lengths in the

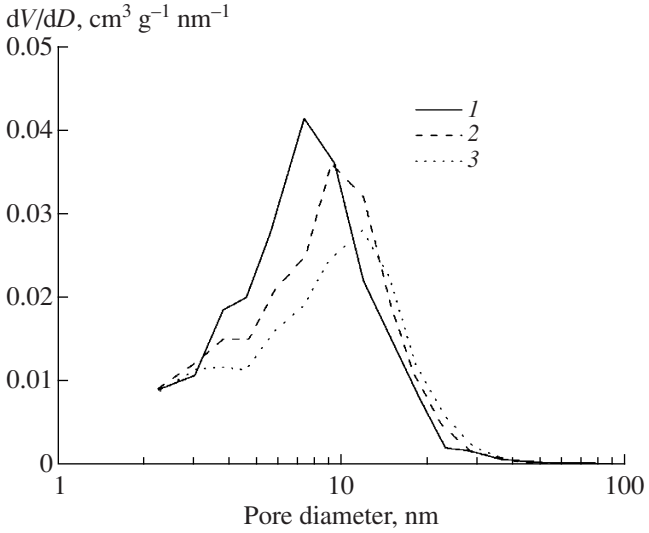

Fig. 3. Differential distribution of the mesopore volume over pore size for V/Ti = (*1*) 0.025, (*2*) 0.050, and (*3*) 0.100.

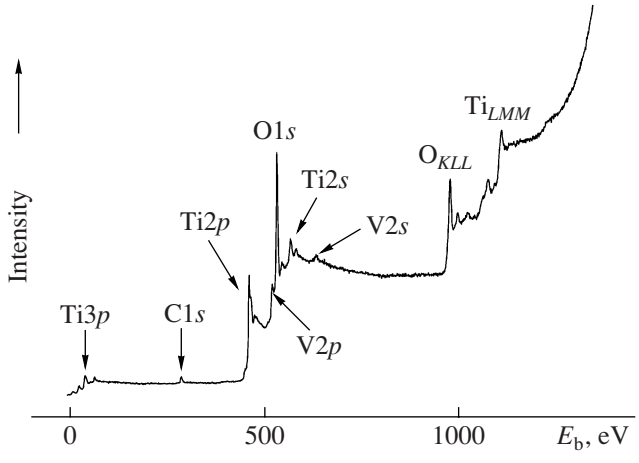

Fig. 4. Survey photoelectron spectrum of the V/Ti = 0.100 oxide.

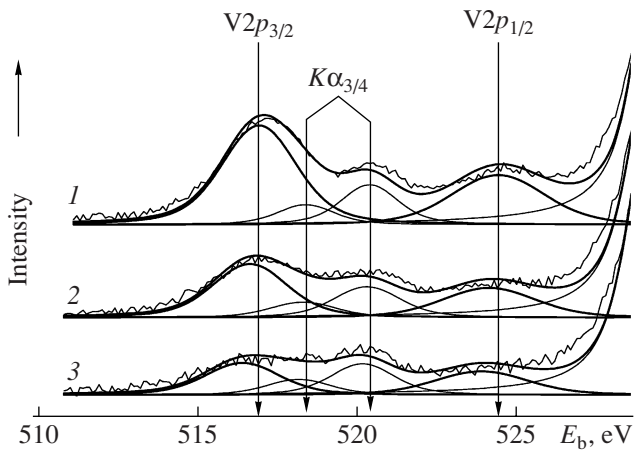

Fig. 5. V2*p* spectra of the V/Ti = (*1*) 0.100, (*2*) 0.050, and (*3*) 0.025 mixed oxides obtained by sol–gel processing. The spectra are normalized to the intensities of the corresponding Ti2*p* spectra.

VO_6 octahedra show themselves as broad medium-intensity bands between 1160 and 1118 cm^{-1}. The double bonds V^{5+}=O and V^{4+}=O give rise to a broad band at 1071 and 980 cm^{-1}, respectively. The shoulder near 925 cm^{-1} indicates the existence of Ti–O…H and V–O…H groups. This solid solution contains water molecules, which are likely adsorbed on its surface. The bending vibrations of these molecules show themselves as a strong broad band at 1634 cm^{-1}.

A comparison between the IR spectrum of the sol–gel sample and the spectrum of vanadium oxide supported on the anatase surface (Fig. 6) shows that, in the former case, V_2O_5 is dissolved in the anatase bulk. The V=O stretching band, which occurs at 1023 cm^{-1} for V_2O_5, is shifted to a higher frequency of 1071 cm^{-1} for the sol–gel sample. This accompanied by an increase the vibration frequencies of the Ti–O and Ti–O–Ti bonds.

In the case of the conventional supporting of V_2O_5 on the anatase surface [4] followed by heat treatment, the formation of solutions is incomplete (Fig. 6) and most of the vanadium oxide is unreacted. This is indicated by the V^{5+}=O stretching band at 1023 cm^{-1}, which coincides with the same band for V_2O_5 (ν(V=O) = 1022 cm^{-1}). Furthermore, this sample is almost free of oxygen–hydrogen groups (H_2O and OH^-). According to IR spectroscopic data, mixed oxides of titanium and vanadium obtained by sol–gel processing contain considerable amounts of molecular water and OH groups.

The fact that vanadium atoms (which are the main active sites) occupy different crystallographic positions in the TiO_2 structure is a significant factor in the catalytic activity of the solid solutions. Figure 7 presents the results obtained for chlorobenzene oxidation in the presence of the mixed oxides. It was found that, as the vanadium content of titanium dioxide is increased, the

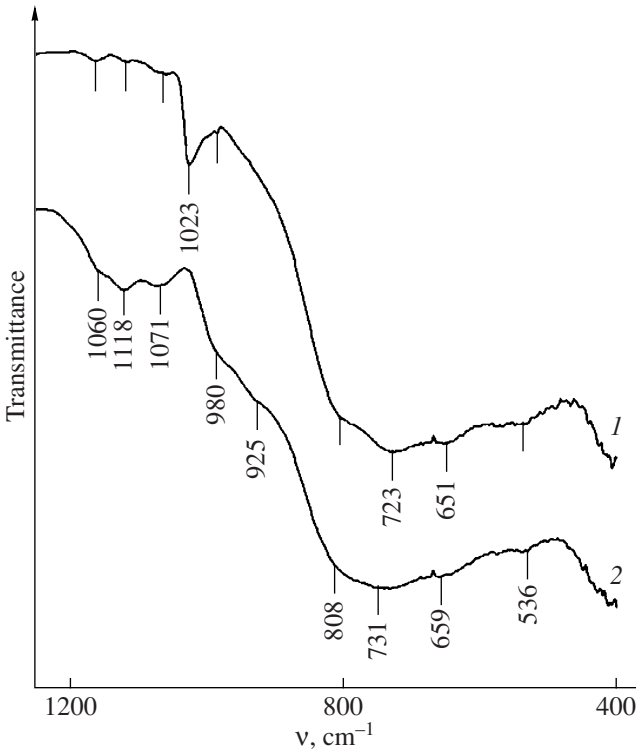

Fig. 6. IR spectra of the V/Ti = 0.100 oxide: (*1*) sample obtained by sol–gel processing; (*2*) sample obtained by the supporting of V_2O_5 onto the TiO_2 surface.

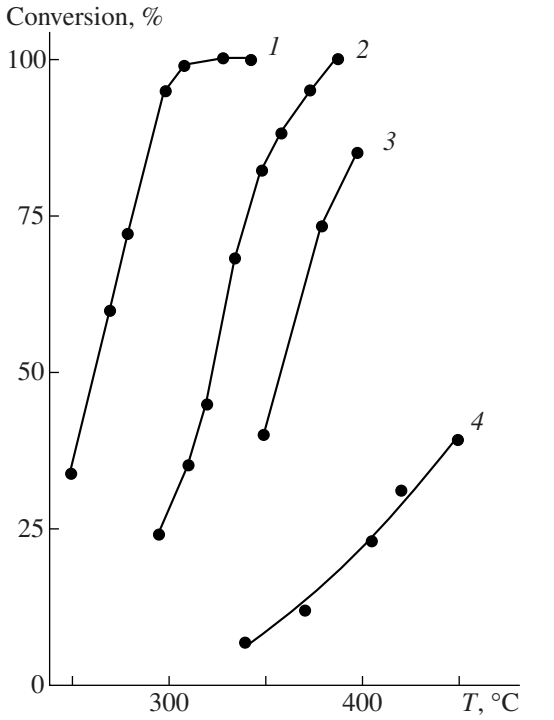

Fig. 7. Temperature dependence of chlorobenzene conversion in the presence of mixed oxides: (*1–3*) sol–gel samples with V/Ti = (*1*) 0.100, (*2*) 0.050, and (*3*) 0.025; (*4*) V/Ti = 0.100 sample obtained by the supporting of V_2O_5 onto the TiO_2 surface.

catalytic activity of the sol–gel solid solutions increases and the 100% chlorobenzene conversion temperature decreases from 430 to 310°C. These oxides show a better catalytic performance than vanadium oxide supported on the anatase surface. They are much more active, even though their specific surface area is smaller. Therefore, the high catalytic performance of the sol–gel oxides is determined by the vanadium content and is due to their specific structural features (increased V=O bond strength), the increased pore size, and the increased oxygen concentration on the oxide surface.

Thus, anatase solid solutions with V/Ti = 0.025, 0.050, and 0.100 were synthesized by reacting a hydrogen peroxide solution of vanadium with titanium hydroxide (precipitated from a titanyl sulfate solution) followed by calcining the resulting solid at 400–450°C. The highest thermal stability is shown by the V/Ti = 0.025 phase (which turns into anatase only starting at 750°C), whose unit cell parameters are smaller than those of titanium dioxide. For V/Ti = 0.100, the anatase $\longrightarrow$ rutile phase transition begins at 600°C. This material has larger unit cell parameters than the other solid solutions, and this may be the cause of its lower thermal stability. Furthermore, most of the vanadium in this phase is in the pentavalent state. According to IR spectroscopic data, the V^{5+}=O bond in this solid solution is shorter than the same bond in pure vanadium oxide or V_2O_5 supported on TiO_2. The vanadium–titanium mixed oxides prepared by sol–gel processing are catalytically very active in chlorobenzene oxidation. At a GHSV = 20000 h^{-1} and a chlorobenzene concentration of 40×10^{-5} mol/l in air, 100% conversion is achieved at 300–310°C.

ACKNOWLEDGMENTS

This study was supported by the Russian Foundation for Basic Research (grant no. r_Ural 07-03-96067) and by the Russian Academy of Sciences through the Ural and Siberian Branches Integration Project.

REFERENCES

1. Grzybowska-Swierkosz, B., *Appl. Catal., A*, 1997, vol. 157, nos. 1–2, p. 263.
2. Dias, C.R. and Portella, M.F., *Catal. Rev. Sci. Eng.*, 1997, vol. 39, no. 3, p. 169.
3. Krishnamoorthy, S., Baker, J.P., and Amiridis, M.D., *Catal. Today*, 1998, vol. 40, no. 1, p. 39.
4. Graham, J.L., Almquist, C.B., Kumar, S., and Sidhu, S., *Catal. Today*, 2003, vol. 88, nos. 1–2, p. 73.
5. Lomnicki, S., Lichtenberger, J., Xu, Z.T., Waters, M., Kosman, J., and Amiridis, M.D., *Appl. Catal., B*, 2003, vol. 46, no. 1, p. 105.
6. Cauqui, M.A. and Rodriques-Izquierdo, J.M., *J. Non-Cryst. Solids*, 1992, vols. 147–148, p. 724.
7. Maciejewski, M., Tschudin, S., Wokaun, A., and Baiker, A., *J. Catal.*, 1994, vol. 149, no. 2, p. 326.
8. Rodella, C.B. and Masteralo, V.R., *J. Phys. Chem. Solids*, 2003, vol. 64, no. 5, p. 833.
9. Gregg, S.J. and Sing, K.S.W., *Adsorption, Surface Area, and Porosity*, London: Academic, 1967.
10. *Handbook of Photoelectron Spectroscopy*, Wagner, C.D., Riggs, W.M., Davis, L.E., Moulder, J.F., and Muilenberg, G.E., Eds., Eden Prairie, Minn.: Perkin-Elmer, 1978.
11. Shirley, D.A., *Phys. Rev. B: Condens. Matter.*, 1972, vol. 5, no. 12, p. 4709.
12. Stakheev, A.Y., Shpiro, E.S., and Apijok, J., *J. Phys. Chem.*, 1993, vol. 97, no. 21, p. 5668.
13. Sleigh, C., Pijpers, A.P., Jaspers, A., Coussens, B., and Meier, R.J., *J. Electron Spectrosc. Relat. Phenom.*, 1996, vol. 77, no. 1, p. 41.
14. Casaletto, M.P., Kaciulis, S., Lisi, L., Mattogno, G., Mezzi, A., Patrono, P., and Ruoppolo, G., *Appl. Catal., A*, 2001, vol. 218, nos. 1–2, p. 129.
15. Sawatzky, G.A. and Post, D., *Phys. Rev. B: Condens. Matter.*, 1979, vol. 20, no. 4, p. 1546.